MOBILITY OF NANOFLUIDS IN POROUS MEDIA

Christos D. Tsakiroglou[1], Sofia Antimisiaris[1,2], Dimitra Tzavara[1,2], Katerina Terzi[1], Christos Aggelopoulos[1]

[1]Foundation for Research and Technology Hellas – Institute of Chemical Engineering Sciences, Stadiou Str., Platani, P.O.Box 1414, 26504 Patras, Greece

[2]Department of Pharmacy, University of Patras, 26504 Patras, Greece

This paper was prepared for presentation at the International Symposium of the Society of Core Analysts held in Avignon, France, 8-11 September, 2014

ABSTRACT

The overall scientific objective of the proposed work is a deeper understanding of nanoparticles (NP) activity and fate in porous media (e.g. stability, transport, agglomeration, reactivity) so that the in situ pollutant remediation efficiency in soils and groundwater is maximized, and the most efficient nanofluids for pilot-scale studies are suggested. Stable nanofluids will be developed by modifying the surface of zero valent iron nanoparticles (nZVI) with adequately selected coatings (e.g. polyelectrolytes) that optimize their colloidal stability, longevity and reactivity. Protocols are developed for the encapsulation of nanofluids in nanoliposomes which are commonly used in drug delivery and are now tested as vehicles for the safe delivery of NP throughout the pore space of a glass-etched pore network and hydrophobic pollutant (n-C_{12}) targeting. In order to assess the capacity of nanoliposomes to break-up and release NP during their travel through the porous medium, a fluorescent dye (calcein) is entrapped in liposomes and its concentration breakthrough curves are measured under varying conditions of flow velocity, liposome concentration, and liposome membrane integrity.

INTRODUCTION

Recently, attention has been paid on the injection of new types of fluids, called "nanofluids", for secondary and tertiary oil recovery [1]. The term of "nanofluid" (NF) is used to describe a suspension resulting from dispersing nanometer-sized materials (nanoparticles, nanofibers, nanorods, nanosheets, nanotubes) in base fluids [1]. When a nanofluid is injected in a porous medium, the improved oil recovery may be associated with changes caused on pore-wall wettability [2] or fluid interfacial tension [3] by nanoparticles. Visualization studies of the immiscible displacement of crude oil by silica nanofluid [2] indicated the wettability alteration and creation of wetting films along the pore-walls of an initially oil-wet porous medium. The size of nanoparticle crystallites is of key importance for the efficiency of secondary/tertiary oil recovery process [4]. Although nanoparticles decrease the interfacial tension and alter wettability, their effectiveness may be questionable in low permeability sandstones due to pore blockage

and reduction of permeability [5]. Investigation of the wetting and spreading of nanofluids on solid surfaces have revealed that the small size and high concentration of silica nanoparticles along with the low contact angle favor the dynamic spreading of nanofluid along the solid surface [6].

Moreover, significant progress has been done on investigating the in situ remediation of contaminated porous media (e.g. soils, sediments, and aquifers) by injecting nanofluids [7]. In spite of the great deal of work done for the in situ remediation of dissolved pollutants with nZVI [8], little progress has been made toward delivery of nZVI to non-aqueous phase liquid (NAPL) source zones. Delivering nZVI to the DNAPL/water interface can potentially increase the rate of DNAPL reduction and the efficient usage of Fe^0 for reductive dechlorination [9]. The dechlorination rate is typically first order with respect to pollutant concentration, and hence, the rate of DNAPL dechlorination can be limited by the availability of dissolved contaminant [10]. Nonetheless, the regions of maximum dissolved contaminants that are most amenable to nZVI targeting are found in the DNAPL source zone (trapped ganglia). Various modifications of nZVI have been suggested to enhance NAPL targeting: (i) nZVI modified by an amphiphilic triblock copolymer that contained polyanionic blocks to stabilize nZVI in suspension and a hydrophobic poly (methyl methacrylate) block to drive nanoparticle adsorption to the NAPL/water interface [11]; (ii) water-in-oil emulsions where nZVI was suspended in the water droplets stabilized by food-grade surfactants [12]; (iii) multifunctional nZVI-silica nanocomposites capable to adsorb to a DNAPL/water interface [13]. (iv) microscale carbonyl iron powder suspensions modified with anionic homopolymers [14]. In macroscopic numerical models of nanoparticle transport in porous media, a variety of solid-liquid mass-transfer mechanisms (e.g. particle attachment/ detachment/ blocking/ ripening, mechanical filtration, straining, etc) are commonly described as exchange terms [15]. NZVI particles for groundwater remediation are engineered with surface coatings to inhibit aggregation, decrease their adhesion to solid surfaces, increase their mobility in the subsurface, and target specific pollutants [16].

In the present work, a fluorescent tracer (calcein) is encapsulated into nanoliposomes which are injected in suspension mode in a glass-etched pore network containing oil ganglia at residual saturation. The controlled delivery of nanofluid at hydrophobic target (oil ganglia/water interfaces) is attained by the adjustment of the flow velocity, the liposome concentration, and integrity of liposome membrane. The tracer concentration breakthrough curves are determined by fluorescence intensity measurements and used to specify the conditions optimizing the liposome membrane disruption within the porous medium. In this manner, the conditions favoring the controlled nZVI deposition on the oil/water interfaces within the porous medium will be identified.

METHODS AND MATERIALS

Photolithography was used to fabricate an artificial large 2-D pore network by etching mirror image patterns (Fig.1a) on two glass plates with hydrofluoric acid, and sintering the pre-aligned etched plates in a programmable furnace. The porous medium model has

been used in two-phase flow and hydrodynamic dispersion studies [17, 18] and its pore space characteristics are shown in Table 1.

Liposomes are predominantly composed of amphiphilic molecules, mainly phospholipids. Because of their amphiphilic character, phospholipids have a strong tendency to form lamellar bilayer structures such as membranes or liposomes in presence of water (Fig.2). Liposomes are prepared by using various procedures where the water soluble (hydrophilic) material is entrapped by using aqueous solution of these materials as hydrating fluid or by adding drug/drug solution at some stage during the preparation of the liposomes. The lipid soluble (lipophilic) materials are solubilized in the organic solution of the constitutive lipid and then evaporated to a dry drug containing lipid film, followed by its hydration. These methods involve the loading of the entrapped agents before or during the manufacturing procedure (passive loading). However, certain type of compounds with ionisable groups, and those which display both lipid and water solubility, can be introduced into the liposomes after the formation of intact vesicles (remote loading) [19]. When preparing liposomes with mixed lipid composition, the lipids must first be dissolved and mixed in an organic solvent to assure a homogeneous mixture of lipids. Typically lipid solutions are prepared at concentration 10-20 mg lipid/ml of organic solvent, although higher concentrations may be used if the lipid solubility and mixing are acceptable. Once the lipids are thoroughly mixed in the organic solvent, the solvent is removed to yield a lipid film. For small volumes of organic solvent (<1mL), the solvent may be evaporated using a dry nitrogen or argon stream in a fume hood. For larger volumes, the organic solvent should be removed by rotary evaporation yielding a thin lipid film on the sides of a round bottom flask. The lipid film is thoroughly dried to remove residual organic solvent by placing the vial or flask on a vacuum pump overnight. Hydration of the dry lipid film is accomplished simply by adding an aqueous medium to the container of dry lipid followed by agitation. The temperature of the hydrating medium should be above the gel-liquid crystal transition temperature, T_c, of the lipid. After addition of the hydrating medium, the lipid suspension should be maintained above the T_c during the hydration period. Disruption of lipid suspensions using sonic energy (sonication) typically produces small, unilamellar vesicles (SUV) with diameters in the range of 15-150nm. The most common instrumentation for preparation of sonicated particles is bath and probe tip sonicators. Mean size and distribution is influenced by composition and concentration, temperature, sonication time and power, volume, and sonicator tuning. The lipid composition was phosphatidylcholine (DSPC) / cholesterol (Chol)= 2:1 mol/mol, and liposomes were prepared by thin film hydration (hydrated with a calcein aqueous solution) and probe sonication (the lipid suspension should begin to clarify to yield a slightly hazy transparent solution) to encapsulate a small hydrophilic fluorescent dye (calcein). Liposomes were dispersed in phosphate buffered saline (PBS: the concentrations were fixed to NaH_2PO_4 1.44g/L, KH_2PO_4 0.24g/L NaCl 8g/L, KCl 0,2g/L and the pH was raised to 7.4). The lipid content was determined using Stewart's method ($FeCl_3.6H_2O$ / NH_4SCN). The release of calcein from liposomes was used as a measure of liposome membrane integrity. The latency percentage (L) was

calculated by using the fluorescence intensity (FI) measurements (λ_{ex}=470nm, λ_{em}=520nm, 25°C), according to

$$L = \frac{c_f FI_{AT} - FI_{BT}}{c_f FI_{AT}} X100 \quad (1)$$

where FI_{BT} and FI_{AT} are the measured FI values before and after the addition of Triton X-100 which is a nonionic surfactant used to disorganize liposomal dispersions, and c_f=1.1 is a correction coefficient due to dilution.

RESULTS AND DISCUSSION

Nanoliposomes (DSPC:CHOL=2:1, mean size=150nm) encapsulating calcein were prepared at concentration 1mg/ml (L= 96.4%) in buffer PBS and were tested in the glass-etched pore network. Initially, the pore network was occupied completely with red-colored n-C_{12} which was displaced by the buffer at a flow rate 0.1mL/min, using a syringe pump. Once the system reached at residual n-C_{12} saturation (Fig.1b), the liposome suspension was injected at flow rate 0.025 mL/min and effluent was collected continuously from the outlet to determine the percentage of calcein released from liposomes by fluorescence intensity measurements. 4 mL of buffer was added in 30 μL of each effluent sample and the FI_{BT} value was measured. Then 400 μL of X-Triton (1% w/w) was added in the sample and the FI_{AT} value was measured. The n-C12 didn't appear any sensible fluorescence intensity. Preliminary results from 2 sets of measurements revealed that, at late times, only a small percentage of the nanoliposomes released the calcein and the majority of outflowing nanoliposomes remain unaltered (Table 2). Therefore, experiments must be performed at lower flow rates (longer retention times) by using smaller nanoliposome concentrations and softer membranes to facilitate membrane disruption and tracer release.

ACKNOWLEDGEMENTS

The research is co-financed by the European Union (European Social Fund-ESF) and Greek national funds in the context of the action "EXCELLENCE II" of the Operational Program "Education and Lifelong Learning" (project: "Optimizing the properties of nanofluids for the efficient in situ soil remediation-SOILREM").

REFERENCES

1. Ehtesabi, H., M.M. Ahadian, V. Taghikhani, and M.H. Ghazanfari. Enhanced Heavy Oil Recovery in Sandstone Cores Using TiO2. *Energy Fuels* (2014) **28**, 423−430.
2. Maghzi, A., S. Mohammadi, M.H. Ghazanfari, R. Kharrat, M.Masihi. Monitoring wettability alteration by silica nanoparticles during water flooding to heavy oils in five-spot systems: A pore-level investigation. *Exper. Thermal and Fluid Sci.* (2012) **40**, 168-176.

3. Suleimanov, B.A., F.S. Ismailov, E.F. Veliyev Nanofluid for enhanced oil recovery. *J. Pet. Sci. Eng.* (2011) **78**, 431-437.
4. Zaid, H.M., N. Yahya, N. Rasyada, A. Latiff. The Effect of Nanoparticles Crystallite Size on the Recovery Efficiency in Dielectric Nanofluid Flooding. *J. Nano Research* (2013) **21**, 103-108.
5. Handraningrat et al., "A coreflood investigation of nanofluid enhanced oil recovery in low-medium permeability berea sandstone", *Proceed. of 2013 SPE Int. Symp. On Oilfield Chemistry*, Apr. 8-10, The Woodlands, TX (2013).
6. Kondiparty, K., A. Nikolov, S. Wu, and D. Wasan. Wetting and Spreading of Nanofluids on Solid Surfaces Driven by the Structural Disjoining Pressure: Statics Analysis and Experiments. *Langmuir* (2011) **27**, 3324-3335.
7. Cundy, A.B., L. Hopkinsona, R.L.D. Whitby. Use of iron-based technologies in contaminated land and groundwater remediation: a review. *Sci. Total Environ.* (2008) **400**, 42–51.
8. Tratnyek, P.G., and R.L. Johnson. Nanotechnologies for environmental cleanup. *Nanotoday* (2006) **1**, 44-48.
9. Liu, Y., S.A. Majetich, R.D. Tilton, D.S. Sholl, and G.V. Lowry. *Environ. Sci. & Technol.* (2005) **39**, 1338-1345.
10. Yan, W., H.-L. Lien, B.E. Koel, and W.-X. Zhang. Iorn nanoparticles for environmental clean-up: recent developments and future outlook. *Environ. Sci.: Processes & Impacts* (2013) **15**, 63-77.
11. Saleh, N., T. Pherat, K. Sirk, B. Dufour, J. Ok, T. Sarbu, K. Matyjazewski, R.D. tilton, and G.V. Lowry. Adsorbed triblock copolymers deliver reactive iron nanoparticles to the oil/water interface. *Nano Lett.* (2005) **5**, 2489-2494.
12. Quinn, J., C. Geiger, C. Clausen, K. Brooks, C. Coon, S. O'Hara, T. Krug, D. Major, W.-S. Yoon, A. Gavaskar, T. Holdsworth. Field demonstration of DNAPL delagogenation using emulsified zero-valent iron. *Environ. Sci. & Technol*. (2005) **39**, 1309-1318.
13. Zhan, J., B. Sunkara, L. Le, V.T. John, J. He, G.L. Mcpherson, G. Piringer, and Y. Lu. Multifunctional colloidal particles for in situ remediation of chlorinated hydrocarbons. *Environ. Sci. Technol.* (2009) **43**, 8616-8621.
14. Bishop, E.J., D.E. Fowler, J.M. Skluzacek, E. Seibel, and T.E. Mallouk. Anionic homopolymers efficiently target zerovalent iron particles to hydrophobic contaminants in sand columns. *Environ. Sci. Technol.* (2010) **44**, 9069-9074.
15. Tosco, T., and R. Sethi. Transport of non-newtonian suspensions of highly concentrated micro- and nanoscale iron particles in porous media: a modeling approach. *Environ. Sci. Technol.* **44**, 9062-9068 (2010).
16. Crane, R.A., and T.B. Scott. Nanoscale zero-valent iron: future prospects for an emerging water treatment technology. *J. Haz. Mat.* (2012) **211-212**, 112-125.
17. Theodoropoulou, M., V. Karoutsos, C. Kaspiris, and C.D. Tsakiroglou. A new visualization technique for the study of solute dispersion in porous media models. *J. Hydrology* (2003) **274**, 176-197.
18. Tsakiroglou, C.D., M.A. Theodoropoulou, V. Karoutsos, and D. Papanicolaou. Determination of the effective transport coefficients of pore networks from transient

immiscible and miscible displacement experiments. *Water Resources Research* (2005) **41(2)**, W02014.

19. Skouras, A., S. Mourtas, E. Markoutsa, M.-C. de Golstein, C. Wallon, S. Catoen, S.G. Antimisiaris. Magnetoliposomes with high USPIO entrapping efficiency, stability and magnetic properties. *Nanomedicine: Nanotechnology, Biology and Medicine* (2011) **7**, 572-579.

Table 1. Structural properties of the model porous medium

Dimensions	Total pore cross-sectional area, A_p (m^2)	Areal porosity	Mean pore width, W_p (μm)	Mean pore depth, D_p (μm)	Pore length, L_p (μm)	Permeability, k (Da)
10.3cm X 14.5cm	$5.9x10^{-6}$	0.65	774	125	1840	19.6

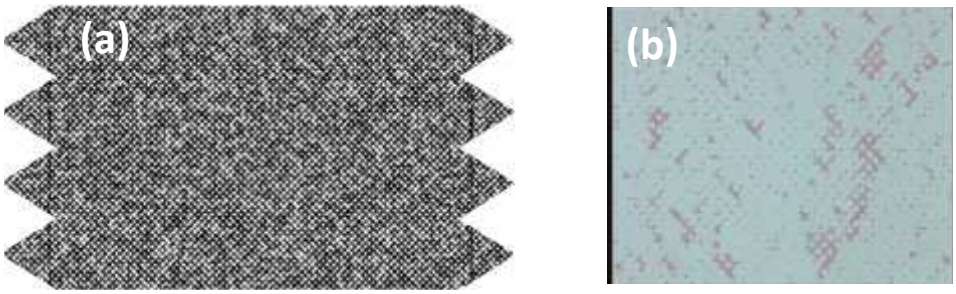

Figure 1. (a) Pattern of 2-D pore network. (b) Injection of liposome suspension at residual n-C_{12} saturation.

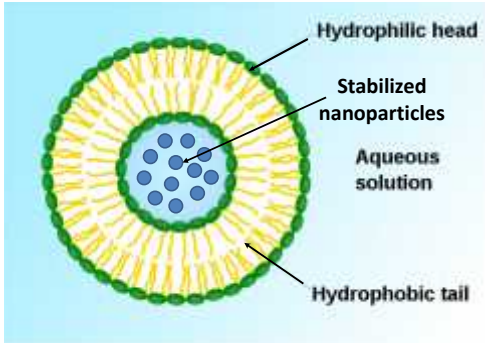

Figure 2. A liposome as a spherical vesicle with lipid bilayers encapsulating nanoparticles.

Table 2. Latency percentage in effluent as a function of time

Time interval, Δt (min)	**L_{av} (%)**	**Standard deviation (%)**	**L_{av} (%)**	**Standard deviation (%)**
Initial sample	96.99	0.08	96.85	5.21
0-5	50.30	7.45	52.96	7.36
5-10	40.56	6.71	27.19	6.58
10-20	62.10	22.0	36.42	7.22
20-40	90.03	0.91	92.24	0.40
40-70	92.09	0.86	92.78	0.49
70-100	96.00	0.33	94.59	0.15